SPECIAL REQUIREMENTS FOR QA IN MAMMOGRAPHY WITH RESPECT TO CR-SYSTEMS

Professor: Dr. Johann Hummel

Fachhochschule Technikum Wien

Author: Laura Rodríguez Larumbe

Acknowledgements

First of all I would like to thank the Technikum Fachhochschule Wien for giving me the opportunity to study at this university.

I would also like to thank the whole team MED UNI Wien for letting me use their laboratories and their team.

I especially would like to thank Mr. Hummel for supporting me, guide me and teach me along the period of this project.

INDEX

I. RESUMEN & ABSTRACT

RESUMEN

En este trabajo final de máster se exponen las mediciones y los resultados obtenidos al realizar una serie de mamografías en el hospital general de Viena (AKH, Allgemeines Krankenhaus der Stadt Wien). Para centrar el tema se hace un recorrido a través del cáncer de pecho, desde el significado de cáncer hasta la explicación detallada de cada experimento realizado, el resultado obtenido y las conclusiones que se han conseguido.

Los resultados obtenidos en papers anteriores para un tamaño de pecho de 50mm, se usan para comparar la efectividad y valorar el uso del ratio de contaste ruido (CNR) y/o del ratio de señal ruido (SNR) a la hora de analizar las imágenes obtenidas para pechos de 60 y 70mm.

Como conclusión se puede afirmar que los resultados obtenidos son aceptables para este tamaño de pechos.

Sin embargo se deberán hacer más mediciones a fin de corroborar que el método es totalmente válido.

ABSTRACT

This Master's Thesis presents the measurements and the results obtained by performing a series of mammograms in the Vienna General Hospital (AKH, Allgemeines Krankenhaus der Stadt Wien). The beginning of the issue is a journey through breast cancer, since the meaning of cancer till the detailed explanation of each experiment, the results that we obtained and the conclusions that we have been made.

The results obtained in previous papers for a 50 mm size of breast, are used to compare and evaluate the effectiveness of the use of Contrast to Noise Ratio (CNR) and / or the Signal to Noise Ratio (SNR) when we are analyzing the images obtained for breasts for 60 and 70mm size.

In conclusion we can say that the results are acceptable for this size of breasts.

However more measurements should be made in order to confirm that the method is completely valid.

II. BREASTCANCER

Breast cancer is an uncontrolled growth of breast cells.

Cancer occurs as a result of mutations, or abnormal changes, in the genes responsible for regulating the growth of cells and keeping them healthy. The genes are in each cell's nucleus, which acts as the "control room" of each cell. Normally, the cells in our bodies replace themselves through an orderly process of cell growth: healthy new cells take over as old ones die out. But over time, mutations can "turn on" certain genes and "turn off" others in a cell. That changed cell gains the ability to keep dividing without control or order, producing more cells just like it and forming a tumor.

A tumor can be benign (not dangerous to health) or malignant (has the potential to be dangerous). Benign tumors are not considered cancerous: their cells are close to normal in appearance, they grow slowly, and they do not invade nearby tissues or spread to other parts of the body. Malignant tumors are cancerous. Left unchecked, malignant cells eventually can spread beyond the original tumor to other parts of the body.

The term “breast cancer” refers to a malignant tumor that has developed from cells in the breast. Usually breast cancer either begins in the cells of the lobules, which are the milk-producing glands, or the ducts, the passages that drain milk from the lobules to the nipple. Less commonly, breast cancer can begin in the stromal tissues, which include the fatty and fibrous connective tissues of the breast.

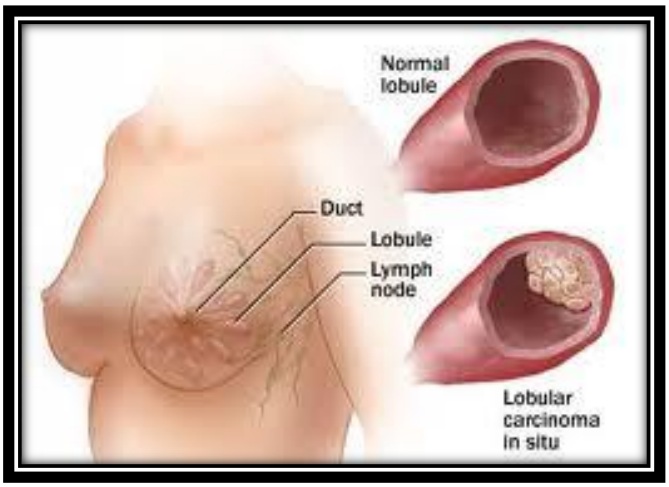

Over time, cancer cells can invade nearby healthy breast tissue and make their way into the underarm lymph nodes, small organs that filter out foreign substances in the body. If cancer cells get into the lymph nodes, they then have a pathway into other parts of the body. The breast cancer’s stage refers to how far the cancer cells have spread beyond the original tumor.

Breast cancer is always caused by a genetic abnormality (a “mistake” in the genetic material). However, only 5-10% of cancers are due to an abnormality inherited from our mother or father. About 90% of breast cancers are due to genetic abnormalities that happen as a result of the aging process and the “wear and tear” of life in general.

There are steps every person can take to help the body stay as healthy as possible and lower risk of breast cancer or a breast cancer recurrence (such as maintaining a healthy weight, not smoking, limiting alcohol, and exercising regularly).

III. MAMOGRAMM

A mammography examination is called a mammogram. A mammogram is an x-ray of the breast. It is a specific type of imaging test that uses a low-dose X-rays to examine the breast.

X-ray (radiograph) is a noninvasive medical test that helps physicians diagnose and treat disease. Radiography involves exposing a part of the body to a small dose of ionizing radiation to produce pictures of the inside of the body. X-rays are the oldest and most common form of medical imaging.

When you have a mammogram, a skilled technologist positions and compresses your breast between two clear plates. The plates are attached to a highly specialized camera, which takes two pictures of the breast from two directions. Then the technologist repeats the technique on the opposite breast. For some women, more than two pictures may be needed to include as much tissue as possible.

Mammography can be painful for some women, but for most it is mildly uncomfortable, and the sensation lasts for just a few seconds. Compressing the breast is necessary to flatten and reduce the thickness of the breast. The x-ray beam should penetrate as few layers of overlapping tissues as possible. From start to finish, the entire procedure takes about 20 minutes.

Mammography involves minimal radiation exposure. In fact, the amount of radiation exposure from modern-day mammography machines is much lower than it was in past decades. The American Cancer Society notes that the dose of radiation received during a screening mammogram is about the same amount of radiation a person gets from their natural surroundings (background radiation) in an average 3-month period.

If you've had breast surgery for another reason, such as a benign biopsy or surgery to reduce the size of your breasts, the radiologist will want to know where those scars are in case the scar tissue has to be distinguished from another kind of breast abnormality. If you've had breast cancer surgery, small metal balls will be taped on your skin to mark your scar. Your scar defines the site with the highest risk of recurrence.

At least one radiologist reads the mammogram. A radiologist is a doctor who specializes in analyzing imaging studies of the body to diagnose disease or other problems. Having two radiologists read your mammogram reduces the chance of missing a problem by about 10-15%. Some centers routinely have your mammogram read twice, but this is expensive, and most insurance companies won't pay for it. You can also get a "second opinion" on your mammogram by having the images analyzed by a computer. This is called computer-aided detection ("CAD"). Special computer software reviews the images and marks any areas of suspicion. The radiologist then examines each area and decides if it needs further evaluation.

Mammograms don't prevent breast cancer, but they can save lives by finding breast cancer as early as possible. For example, mammograms have been shown to lower the risk of dying from breast cancer by 35% in women over the age of 50. In women between ages 40 and 50, the risk reduction appears to be somewhat less. Leading experts, the National Cancer Institute, the American Cancer Society, and the American College of Radiology now recommend annual mammograms for women over 40.

Finding breast cancers early with mammography has also meant that many more women being treated for breast cancer are able to keep their breasts. When caught early, localized cancers can be removed without resorting to breast removal (mastectomy).

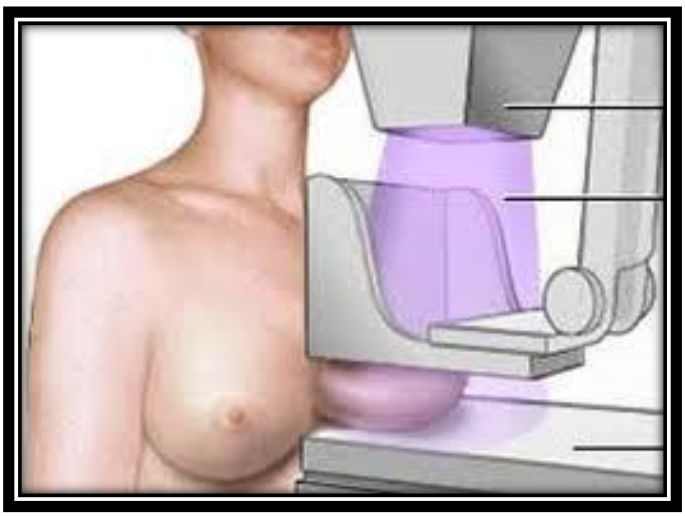

❖ TYPES OF MAMOGRAMM

Differences between screening mammogram and diagnostic mammogram.

Mammograms can be used to look for breast cancer in women who have no signs or symptoms of the disease. This type of mammogram is called a screening mammogram, that is, this procedure is chosen according to the characteristics and preferences of women to find breast cancer when no symptoms. Usually, a mammogram requires two radiographs or images of each breast. The images make it possible to detect tumors that cannot be felt or find microcalcifications (tiny deposits of calcium in the breast) that sometimes are indication of the presence of breast cancer.

Mammograms can also be used to look for breast cancer after having found a lump or other sign or symptom of the cancer. This type of mammogram is called a diagnostic mammogram. Signs of breast cancer include pain, skin thickening, nipple discharge, or a change in breast size or shape, but these signs can also be signs of benign conditions. A diagnostic mammogram can also be used to evaluate changes found during a screening mammogram or to view breast tissue when it is difficult to obtain a screening mammogram because of special circumstances, for example, the presence of breast implants.

Diagnostic mammograms take longer than screening mammograms because more x-rays required obtaining views of the breast from several angles. The technician may magnify a suspicious area to produce a detailed picture to help the doctor make an accurate diagnosis.

Differences between digital mammography and conventional mammography.

There are two main types of mammography: film-screen mammography and digital mammography, also called full-field digital mammography or FFDM.

Both digital and conventional mammography uses X-ray radiation to produce an image of the breast. However, conventional mammography records the image directly on a sheet of film, while digital mammography is a mammography system in which the x-ray film is replaced by solid-state detectors that convert x-rays into electrical signals. The electrical signals are used to produce images of the breast that can be seen on a computer screen or printed on special film similar to conventional mammograms.

This digital information can be enhanced, enlarged or manipulated for further evaluation more easily than information stored on film. Apart from the difference in the form of recording and storing the image, there is no other difference between the two types of mammography.

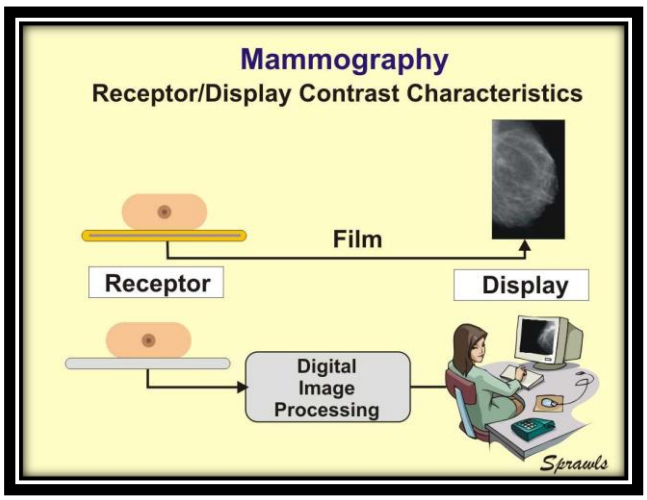

Since digital mammography allows the radiologist adjustment, electronically store and retrieve digital images, digital mammography may offer the following advantages not offered by conventional mammography:

- Medical professionals can share electronically archived images, which facilitates long-distance consultations between radiologists and breast surgeons.
- May more easily notice subtle differences between normal and abnormal tissues.
- Digital images can be manipulated for better views and they can be stored more easily.
- The number of necessary follow-up procedures may be less.
- It may be necessary to repeat or fewer images, which reduces the time of exposure to radiation.
- Digital mammograms deliver about three-fourths of the radiation that film-screen mammograms do.

The disadvantages of digital mammography are that:

- It is more expensive.
- It not as widely available as film-screen mammography.

In January 2000, the FDA (Food and Drug Administration) approved the use of digital mammography. Many studies have shown that film-screen and digital mammography are equally accurate in screening for breast cancer. In September 2005, were published the preliminary results of a large clinical study comparing digital mammography with film mammography. These results revealed no difference between digital and conventional mammography to detect breast cancer in the general population of women in the study. However, the researchers concluded that digital mammography may be more accurate than conventional film mammography in women with dense breasts who are premenopausal or perimenopausal (women who had their last menstrual period within twelve months of their mammograms), have very dense or extremely dense breast tissue or who are under 50 years of age. It is not known whether this accurately will result in a lower risk of dying from breast cancer.

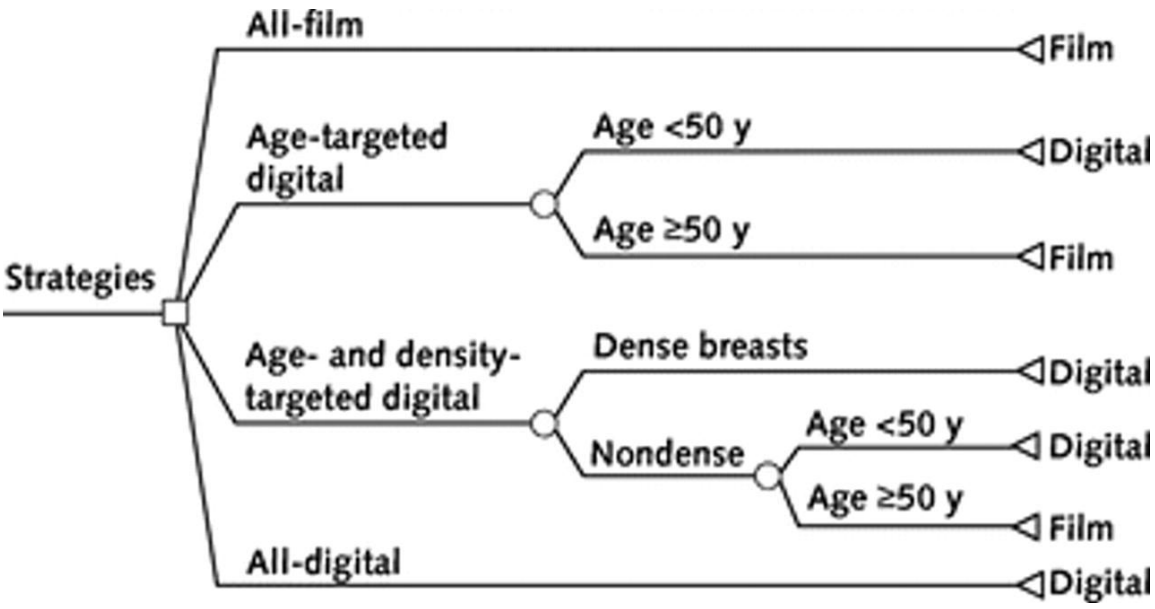

In Some medical professionals recommend that women who have a very high risk of breast cancer, such as those with mutations in BRCA1 (breast cancer type 1)or BRCA2 (breast cancer type 2), digital mammograms are performed instead of conventional, but no study has shown that digital mammograms are superior to conventional mammography for these women.

Digital mammograms can be done only in establishments certified to perform conventional mammography and have received FDA approval to offer digital mammography. The procedure for a mammogram with a digital system is the same as with conventional mammography.

In a film-screen mammogram, the images will be in black and white on large sheets of film. With digital mammography, the images are recorded directly into a computer. The image can then be viewed on a computer screen and specific areas can be enlarged or highlighted. If there is a suspicious area, doctors can use the computer to take a closer look. The images also can be transmitted electronically from one location to another.

In the future, it's expected that digital mammography will become more common. Many imaging centers are now in the process of switching over from traditional film mammography to digital mammography.

❖ WHAT OTHER TECHNOLOGIES ARE BEING DEVELOPED?

Computer-Aided Detection.

Systems computer-aided detection (CAD) uses a digitized mammographic image that can be obtained from either a conventional film mammogram or a digitally acquired mammogram. The computer software then searches for abnormal areas of density, mass, or calcification that may indicate the presence of cancer. The system of computer-aided detection highlights these areas on the images, alerting the radiologist to the need for further investigation.

A study published in the New England Journal of Medicine showed that CAD may falsely suggest suspicious areas of growth in the breast, but may not substantially detect more breast cancer cases. The study reported that for every 100,000 mammograms, 2,985 more false positive mammograms will occur, and five more cancers will be detected. In another recent study published in the Journal of the National Cancer Institute, researchers concluded that the use of CAD did not improve the rate of detecting cancer.

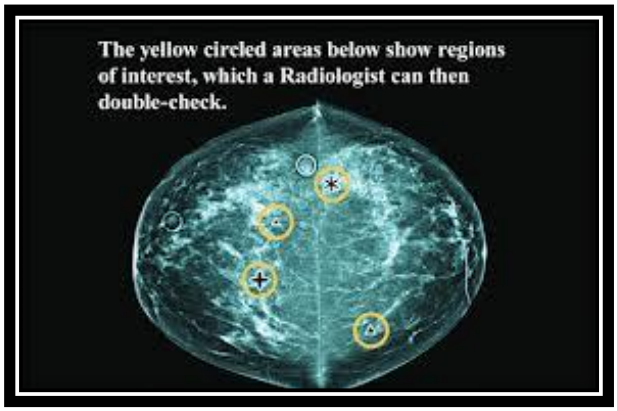

The National Cancer Institute

The National Cancer Institute is supporting the creation of several new technologies to detect breast tumors. This research ranges from methods that are being developed in laboratories to those who are being evaluated in clinical trials. Efforts to improve conventional mammography include digital mammography, magnetic resonance imaging (MRI) and positron emission tomography (PET).

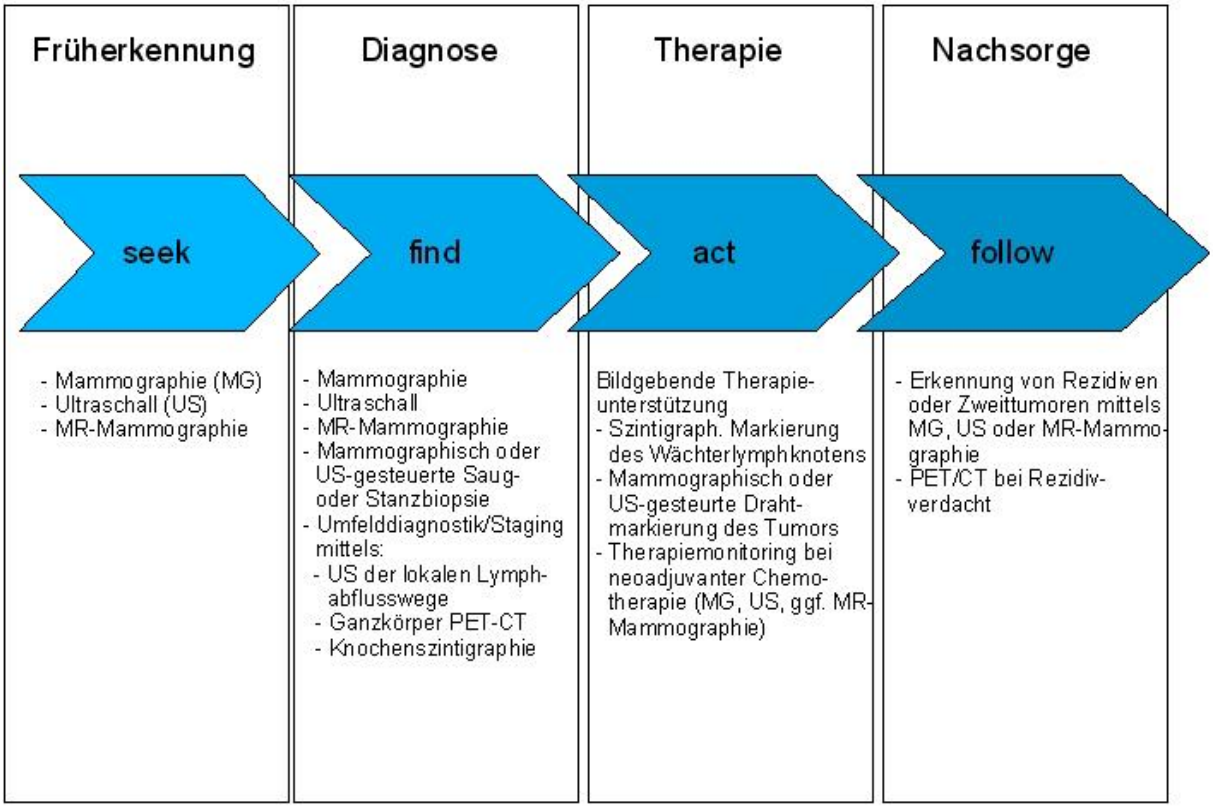

IV. THE ROSE MODEL

Albert Rose (born New York City, 30 March 1910, died on 26 July 1990) was an American physicist, who made major contributions to TV video camera tubes such as the orthicon, image orthicon, and vidicon. Rose was an expert on photoconductivity. He wrote a book "Concepts in photoconductivity and allied problems", which was published by John Wiley & Sons, New York in 1963. He also did research on the visibility of objects in a noisy signal, such as from TV tubes. He found that human could distinguish small objects in noisy images near 100% accuracy if the object brightness differed from the background by 5 or more times the noise standard deviation; this signal-to-noise relationship is known as the Rose Criterion.

In 1946 and 1948, three very important papers by Albert Rose [J. Soc. Motion Pict. Eng. 47, 273 (1946); J. Opt. Soc. Am. 38, 196 (1948); L. Marton, ed. (Academic, New York, 1948)] were published on the role that photon fluctuations have in setting fundamental performance limits for both human vision and electronic imaging systems. The papers were important because Rose demonstrated that the performance of imaging devices can be evaluated with an absolute scale (quantum efficiency). The analysis of human visual signal detection used in these papers (developed before the formal theory of signal detectability) was based on an approach that has come to be known as the *Rose model*.

In spite of its simplicity, the Rose model is a very good approximation of a Bayesian ideal observer for the carefully and narrowly defined conditions that Rose considered. This simple model can be used effectively for back-of-the-envelope calculations, but it needs to be used with care because of its limited range of validity. One important conclusion arising from Rose's investigations is that pixel signal-to-noise ratio is not a good figure of merit for imaging systems or components, even though it is still occasionally used as such by some researchers.

Rose in his seminal publications proposed and described the use of an absolute scale (quantum efficiency) for evaluating imaging system performance, and a simple model of signal detectability by human observers. Rose used a particle-based fluctuations theory to compare realized devices with an ideal device, with the performances of both being assumed to be limited only by photon fluctuations. The images shown in the figure were used by Rose in 1953 to demonstrate the maximum amount of information that can be conveyed by various known numbers of photons.

Rose's papers on assessment of the performance of electronic devices and of the human visual system on an absolute scale came during a time of major technological change. Rose had been an important participant in the development of electronic television camera tubes at RCA since 1935. There had been a very rapid increase in camera sensitivity and a resulting need for evaluation metrics. Rose explored the consequences of the quantum nature of light as the fundamental determinant of performance. This was not a completely new idea; it had already been applied to the study of the limits of human visual system performance.

In 1932, Barnes and Czerny suggested that statistical fluctuations in photon arrival might limit human visual perception. In 1942, Hecht estimated the minimum number of photons necessary to produce a sensation of light in the retina. de Vries estimated effects of photon statistics on contrast sensitivity and acuity. Rose was the first to make complete use of a statistical approach.

Rose's work on noise effects and ultimate limits to sensitivity was concerned with just one of a number of factors limiting image quality. Early evaluations of the imaging properties of photography, television, and optical and visual systems were based on different, non commensurable methods. O. Schade, at RCA, was developing spatialfrequency-dependent measurement techniques, measurement scales, and performance indices that could be used across the entire spectrum of imaging modalities. The results of that work are summarized by examples in his marvelous book Image Quality: a Comparison of Photographic and Television Systems, with a foreword by Rose. Much of Schade's work has been translated into modern signal detection theory notation by Wagner.

Rose's ideas found immediate application in the medical imaging field. In 1948, Coltman described the development of a prototype electronic x-ray image intensification device and pointed out that the images would be impaired by the quantum nature of light. Sturm and Morgan used Rose's concepts and observer model to calculate the expected benefits of electronic intensification in fluoroscopy. They explicitly pointed out the fundamental role that photon statistics would play in limiting the clarity with which fluoroscopic images would be visualized.

The basic ideas of the Rose model are presented here in a slightly different way from that of his publications, to make a number of important distinctions. Rose was considering the detectability of a flat-topped, sharp-edged signal of area, A, in a uniform background. This choice of signal allowed it to be described by either one scalar (the average incremental number of photons, (ΔNs), that represent the signal) or two scalars (the signal contrast, C, and area, A) rather than a function, s(x, y).

Rose described the photon noise by its statistics in a background region with the same area as the signal: the mean number of photons in the area, (Nb), and the variance, σNb2, which equals the mean, since photons have Poisson statistics. It is very important to note, as Rose did, that recorded photons are uncorrelated. For clarity, it is more convenient to use the corresponding mean photon densities, (Δns) extra photons per unit area for the signal, and (nb) expected photons per unit area for the background. Using a signal contrast, C = (ΔNs)/ (Nb) = (Δns)/ (nb), Rose defined SNR with the equation:

$$SNR_{Rose} = \frac{Mean\ signal}{\sigma Nb} = \frac{\Delta Ns}{\sqrt{Nb}} = \frac{A*(\Delta ns)}{\sqrt{A*(nb)}} = C*\sqrt{A(nb)}$$

Now consider the Rose SNR definition in the context of SDT. Two assumptions are necessary to compare the Rose model based on Poisson noise with the previous SDT models based on Gaussian noise. The Rose model neglects the fact that noise in the potential signal location has unequal variances for the signal-present and signal absent cases. If the signal is present, the variance will equal the mean total, ($\Delta N_s + N_b$). So we need to assume that DNs is very small compared with Nb. Hence the Rose model is an approximation that is valid only in the limit of low-contrast signals. The photon noise has a Poisson distribution, whereas the above SDT approach was based on a Gaussian distribution. We need to assume that photon densities are large enough that Poisson noise can be approximated by Gaussian noise with the same mean and variance.

Other aspects of the Rose model fit conditions of the above SDT model for uncorrelated noise. Rose used completely defined signals at known locations on a uniform background for his experiments and analysis, so the SKE and BKE constraints of the simple SDT analysis were satisfied. He assumed perfect use of prior information about the signal. He used a flat-topped signal at the detector plane (which is only possible when there is no imaging system blur). This assumption meant that integration of photon counts over the known signal area is equivalent to cross-correlation detection. This can be seen by consideration of the following argument. Consider the cross correlation of a signal, s(x, y), and a template, t(x, y), both located at the expected signal location (x = y = 0) in an image with additive, uncorrelated Gaussian noise.

The noise functions with and without the signal are $n_s(x, y)$ and $n_n(x, y)$ with zero mean and spectral density equal to (N0). Let the signal have a flat top and sharp edges (the signal is nonzero only in the range R) with area A and amplitude a above the background. Let the template be an arbitrarily amplified version of the signal, t(x, y) = τs(x, y). To obtains the SNR defined by SDT:

$$(\Lambda_s) - (\Lambda_n) = \left(\frac{1}{N0}\right) \int_{-\infty}^{\infty}\int_{-\infty}^{\infty}[\{s(x,y) + ns\,(x,y) - nn(x,y)\}t(x,y)]dxdy = \left(\frac{a\,\tau}{N0}\right)\iint_R dx\,dy = \frac{a\,\tau A}{N0},$$

$$\sigma\Lambda_s^{\,2} = \sigma\Lambda_n^{\,2} = \left(\frac{1}{N0}\right)^2 \int_{-\infty}^{\infty}\int_{-\infty}^{\infty}[n(x,y)2\ t\ (x,y)2]dxdy = \left(\frac{\tau}{N0}\right)^2 \int\int_R [n(x,y)2]dxdy = \frac{\tau\ 2N0A}{N02},$$

$$SNR^2 = (d')^2 = \frac{(\,(\Lambda s) - (\Lambda n)\,)2}{(1/2)(\sigma\Lambda s2 + \sigma\Lambda n2)} = \frac{\tau\ 2\ a\ 2A2N02}{\tau\ 2\ a\ N03} = \frac{a\ 2A}{N0}$$

The equality of Rose's SNR approximation and the SDT definition of SNR can be shown by use of Rose's definition of contrast and by the fact that N_0 equals (n_b) for Poisson noise:

$$C = \frac{\Delta ns}{nb} = \frac{a}{N0}$$

$$SNR_{Rose} = C^2A\,(n_b) = \left(\frac{a}{N0}\right)^2 AN_0 = \frac{a2A}{N0} = SNR^2.$$

So the Rose model, when limited to this idealized special case, is a very good approximation to the Bayesian ideal observer model. However, it must be used with care to ensure that all the above conditions and assumptions are satisfied. Rose used his model to assess the detectability of signals, in that he asked the question, ‘‘What SNR was required in order to detect a signal?’’ His approach was to use a constant, k, defined as the threshold SNR, and to suggest that the value of k must be determined experimentally.

The signal was expected to be reliably detectable if its SNR were above this threshold. Once k is selected, the corresponding contrast threshold C_T is given by:

$$C_T = \frac{k}{\sqrt{A\,(nb)}}$$

Using this definition of threshold SNR has the unfortunate effect of mixing the measure of relative signal strength (SNR) with the observer’s decision criterion. However, it followed the convention of the day. This threshold SNR concept is still sometimes used by people unfamiliar with SDT.

V. CDMAM

❖ INTRODUCTION

In mammography it is essential that objects with very small contrast and diameter can be distinguished from the background for a reliable diagnosis. Therefore the quality of the technical aspects of the mammography equipment should be monitored at regular time-intervals. This is usually performed by measurement of the physical parameters of the X-ray equipment, screen-film combination, developing process and observation conditions. The main item in quality control however should be assurance of information transfer from the tissue under examination to the radiologist. Therefore the information content of an image should be monitored.

To evaluate the image quality of mammography systems, a contrast-detail phantom was developed, the CDMAM-phantom. With this phantom, which has been adapted from the Burger-Rose phantom (Burger 1950), the threshold contrast of an imaging system is determined as a function of object diameter, by the detection of pairs of low-contrast objects.

The constant improvement of image quality in mammography made it necessary to visualize lower contrast, as well as a higher spatial resolution (smaller objects) at a higher contrast. The CDMAM phantom was modified to facilitate the evaluation of these systems.

The radiographic image obtained from CDMAM be evaluated in the area where the holes are visible, indicating the position of objects. These observations corrections were applied based on the four closest neighbors.

The CDMAM phantom consists of an aluminium base with gold-disks of various thickness and diameter, which is attached to a plexiglass cover. The phantom is delivered with 4 plexiglass plates, each with a thickness of 10mm. The dimensions of phantom and plexiglass plates match the standard mammography film size (180*240mm). It has a matrix of square cells with dots of varying size and contrast. In each of the 205 cells of the matrix one dot is at the center and another is positioned in a randomly selected corner. The observer's task is detection of the dots. Target diameters range from 60µm to 2mm, and thicknesses range from 0.03 and 2 µm of gold.

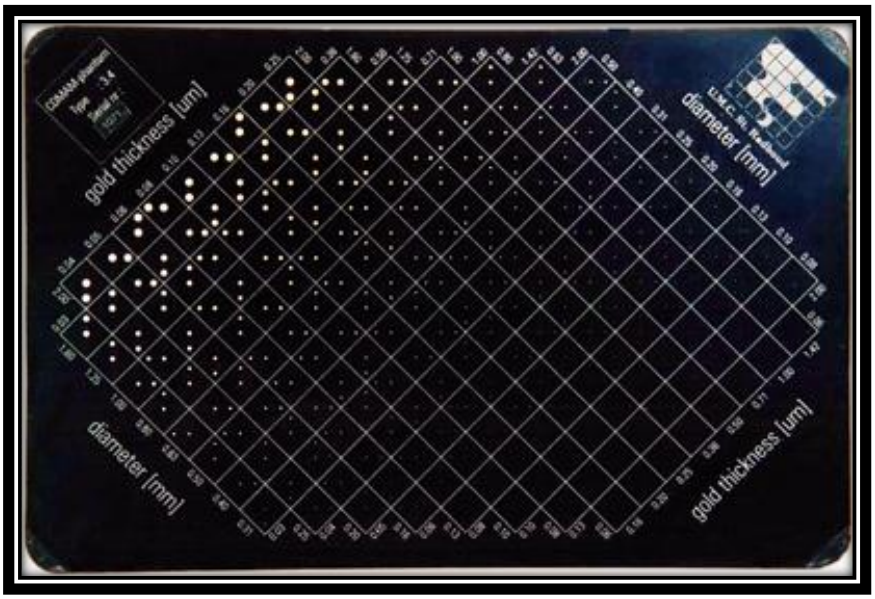

❖ DESCRIPTION OF THE PHANTOM

The aluminium base

The aluminium base consists of Al 1050 (99.5% pure aluminium) and has a thickness of 0.5 mm. The base has been polished and was anodized black.

The disks are arranged in a matrix of 16 rows and 16 columns. The matrix is rotated 45°, to minimize influences of the heel-effect (optical density variations).

Each square contains two identical disks, one in the centre and one in a randomly chosen corner, to allow verification of the detection of each object. Easily memorizable patterns have been avoided. The phantom has been designed such that about half of the disks will be detected by an experienced observer, when state of the art mammography equipment (high contrast film-screen combinations or digital mammography) is used at standard exposure conditions.

The plexiglass cover

The cover consists of a 5 mm thick plexiglass (PMMA) plate. In the cover a cavity with a depth of 2mm has been milled, to accommodate the aluminum base with the gold-disks.

Between the plexiglass cover and the aluminium base a silkscreen printed transparent with X-ray contrasting paint has been placed, showing a grid, the disk thickness and disk diameter. Consequently the X-ray image will show a number of squares arranged in 16 columns and 16 rows, with the disk-diameter shown for each row and the disk-thickness for each column.

The plexiglass plates

The CDMAM-phantom is delivered with 4 plexiglass plates, for the simulation of different breast-thicknesses. The plates have a thickness of 10 mm each and are otherwise of the same dimensions as the phantom. For easy identification in the X-ray image of the number and relative position of any added plates, they are marked in one corner with X-ray contrasting paint.

Gold disk

The disks can deviate slightly from the intended diameter, and will not be exactly circular. Also the thickness of the disks may deviate from the indicated values, mainly due to the gold vaporization profile. Thickness at the centre of the phantom tends to be more, and at the edges less than intended.

The acceptable magnitude of deviations of gold-disk dimensions is related to the thickness, diameter and area step between two consecutive disk rows and columns in the phantom. Generally, deviations appear to become more significant at smaller disk diameters.

❖ DIRECTIONS FOR USE OF THE PHANTOM

To make an X-ray image, the CDMAM-phantom should be positioned on the bucky with the smallest disk-diameters at the thorax side, in combination with one or more plexiglass plates.

Choices have to be made with regard to the exposure technique:

- Tube potential.
- Focal spot size.
- With or without grid.
- Manual or automatic exposure.
- With or without compression plate.

After the film has been processed, the density of the film should be checked. In a series of Contrast-Detail images, all the images should have approximately the same densities in a reference position on the film. After this pre-processing the images can be analyzed in “CDMAM Analyzer“ to determine the Contrast-Detail curve and used for evaluation of the image quality.

CDMAM is considered to be the world gold standard and is described in the European Protocol for quality assurance in Digital Mammography.

❖ APPLICATIONS

- Determination if mammographic images are indicating objects with very low contrast and very small diameter.
- Monitors the image information contact with the Contrast-Detail curve and the spatial resolution.
- Determination of the optimum exposure technique, e.g., by variation of tube potential
- Comparison of image quality at various object thicknesses by variation of the amount of PMMA thickness.
- Characterize the image of digital mammography.
- Comparison of image quality with various film-screen combinations.
- Determination of the optimum background density.
- Comparison of different mammography systems.
- For full-field analog and digital units.

VI. CNR and SNR

CNR: Contrast to Noise Ratio. It is a measure of the detectors ability to distinguish between objects in an image and the image noise.

SNR: Signal to Noise Ratio. It compares the level of the desired signal to the level of background noise. A higher SNR provides a better image.

Image quality at other PMMA thicknesses.

The protocol for digital mammography image quality at other thicknesses than standard thickness is related to the image quality at the standard thickness using Signal-to-Noise Ratio (SNR) and Contrast-to-Noise Ratio (CNR) requirements. The absolute values of SNR and CNR are system dependent (they are dependent on pixel size, for example), therefore limiting values need to be expressed in terms of variation in SNR over the whole range of simulated breast thicknesses and percentage of CNR at standard thickness respectively.

However there are difficulties with this measurement. At this moment three kinds of parameters are used by manufacturers to control image quality in AEC systems: dose to the detector (pixel value), SNR and CNR. Screen-film mammography systems and some digital systems keep dose to the AEC detector constant over the whole range of breast thicknesses (for digital systems this means that pixel value is kept constant), some other systems keep SNR constant and recently a system has been introduced which tries to keep CNR constant.

CNR would be the right measure to quantify image quality at thicknesses other than standard thickness.

CNR should not necessarily be equal across the whole range of breast thicknesses. However, problems arise when setting the CNR value at standard thickness as reference for other thicknesses using the method described in the Protocol for digital mammography. If the CNR at standard thickness is high, CNR at other thicknesses may fail, not because image quality is too low, but because image quality at standard thickness is relatively high. So the method of testing and limiting values needed to be revised.

Nowadays the value of CNR at standard thickness is estimated which would be obtained on a system if this system just complied with the acceptable limiting values of threshold contrast visibility. In the calculation of this minimum CNR level it is assumed that quantum noise is the main source of noise in the system. The calculation is based on the Rose theory, from which can be derived that threshold contrast visibility is inversely related to CNR.

The calculated CNR at the acceptable limiting value of threshold contrast is the lower limit of CNR at standard thickness. Lower limits of CNR at other thickness are related to this value providing sufficient CNR for the whole range of breast thickness.

VII. FIRST STEPS

As Plato said, "The beginning is the most important." And that is why in order to ensure that the data that will be used later are reliable, we performed the following calculations.

Based on the results obtained by members of the AKH (Allgemeines Krankenhaus der Stadt Wien) on the 50mm CDMAM, is found that the calculations for the CNR (70mm) satisfy with the standard, where the CNR (70mm) is higher than the 85% of the CNR (50mm).

Diametro 0,1mm		
	Example 1	
CNR (50mm)	8	Result 
CNR (70mm)	7,2	90%

	Example 2	
CNR (50mm)	12	Result 
CNR (70mm)	7,2	60%

As in the second example the result was not the required, our follow step was to demonstrate that:

$$CNR*T = cte$$

$$CNR_{mes} * T_{mes} = CNR_{th} * T_{th}$$

The value for T_{th} is $T_{th} = 1.68$ according to the protocol.

So we can find CNR_{th} and check with this method, that the result is greater than 85%.

$$CNR_{th} = \frac{CNRmes * Tmes}{Tth} = \frac{12*1}{1,68} = 7,1$$

And so the result is valid now.

Diametro 0,1mm		
	Example 2 - Better	
$CNR_{100\%}$ (50mm)	7,1	Result 
CNR (70mm)	7,2	101%

Once verified that the result was the required the next step is to determine whether the improved model of Rose, which was discussed in previous sections, was the requested. With them was shown that the maximum CNR was lower than the CNR to 100%.

$$CNR_{mes} * T_{mes} = CNR_{100\%} * T_{100\%} \rightarrow \text{Rose model}$$

$$CNR_{mes} * T^{1/2B}_{mes} = CNR_{100\%} * T^{1/2B}_{100\%} \rightarrow \text{Improved Rose model}$$

The $CNR_{100\%}$ is:

$$CNR_{100\%} = \frac{\text{CNRmes} * \text{Tmes}\text{^}(\frac{1}{2B})}{\text{T100\%}\text{^}(\frac{1}{2B})}$$

	CNR (measurement)	T (measurement)	T 100%	B	T^(1/2B) (measurement)	T^(1/2B) 100%	CNR 100%
LIESING	6,3	1,17	1,68	0,72	1,115196	1,433721	4,900350
BRIGITTENAU	6,06	1,31	1,68	0,8	1,183844	1,382988	5,187390
LINHART	6,45	1,475	1,68	0,89	1,244019	1,338376	5,995266

LIESING → $CNR_{grenzwert}$ = 4,525 < 4,900350

BRIGITTENAU → $CNR_{grenzwert}$ = 4,832 < 5,187390

LINHART → $CNR_{grenzwert}$ = 5,743 < 5,995266

When the variable B has a value less than 0.5 as is required by Rose model improved, the result becomes that the limit of CNR is less than CNR100%.

For this we have used B = 0.4

$$CNR_{100\%} = \frac{CNRmes * Tmes\wedge(\frac{1}{0,8})}{T100\%\wedge(\frac{1}{0,8})}$$

In the next table we can observe the results:

	CNR (measurement)	T (measurement)	T 100%	B	T^(1/2B) (measurement)	T^(1/2B) 100%	CNR 100%
LIESING	6,3	1,17	1,68	0,4	1,216837	1,912655	4,008079
BRIGITTENAU	6,06	1,31	1,68	0,4	1,401487	1,912655	4,440431
LINHART	6,45	1,475	1,68	0,4	1,625511	1,912655	5,481673

LIESING → $CNR_{grenzwert}$ = 4,525 > 4,008079

BRIGITTENAU → $CNR_{grenzwert}$ = 4,832 > 4,440431

LINHART → $CNR_{grenzwert}$ = 5,743 > 5,481673

We can say then that the Rose model improved is better than the conventional Rose model.

The next step is therefore to find its parameters “a” and “b”.

$$mAs = KV = a * MPV^{b}$$

To do this we used the data from the database from the AKH (Allgemeines Krankenhaus der Stadt Wien). We took the data for CR where B <0.5, B = 0.4. Most of them corresponded with those investigations that had worked with Fuji or Kodak's brand.

We tried different values of “a” and “b” until the sum of all the results, was as much as possible 0.

After several attempts the results obtained were:

	mAs	MPV	SD	SD^2	mAs	$(mAs-SD)^2$
Kainberger	10	6,59	0,95	0,9	0,949122	7,710E-07
	20	11,49	1,32	1,74	1,284092	1,289E-03
	30	15,95	1,5	2,25	1,534776	1,209E-03
	60	29,44	2,12	4,49	2,141768	4,738E-04
	80	38,07	2,54	6,47	2,463070	5,918E-03
	120	46,8	2,8	7,82	2,755680	1,964E-03
	140	65,26	3,27	10,72	3,301745	1,008E-03
	200	92,09	3,84	14,75	3,981678	2,007E-02
	350	137,8	5,04	25,39	4,957219	6,853E-03
					SUM	**0,038789**

a = 0,340465
b = 0,543726

	mAs	MPV	SD	SD^2	mAs	$(mAs-SD)^2$
Kirchdorf	11	933,503			0,034353	0,001180
	28	933,503			0,034353	0,001180
	56	959,3415	-0,00252	1,7	0,034730	0,001388
	63	1445,237	-0,00371	2990,6	0,040916	0,001991
	110	2216,013	-0,00572	4669,1	0,048545	0,002945
	160	3138,182	-0,00817	6651,4	0,055794	0,004091
	220	4021,02	-0,01054	8906,8	0,061610	0,005206
	280	4567,761	-0,01203	10310,5	0,064833	0,005908
	320	5597,563	-0,01485	13479,9	0,070326	0,007256
					SUM	**0,028784**

a = 0,00223
b = 0,4

	mAs	MPV	SD	SD²	mAs	(mAs-SD)²
Mistelbach	2,8	577	0	0	54,558471	2976,627
	5	577	0	0	54,558471	2976,627
	10	577	0	0	54,558471	2976,627
	22	588,65	25,67	658,92	55,478913	888,571
	45	1283,8	114,32	13067,92	106,548929	60,390
	90	2236,67	175,71	30875,58	169,566025	37,748
	180	3895,7	273,5	74801,01	269,790942	13,757
	280	7083,49	456,56	205691,72	444,988092	133,909
	360	12399,14	695,6	483855,09	710,960177	235,935
	560	22396,21	1170,06	1369052	1166,156693	15,236
					SUM	**1385,54624**

a = 0,266641
b = 0,836939

	mAs	MPV	SD	SD²	mAs	(mAs-SD)²
Rachinger	110	1688,55	81,99	6722,62	81,9420119	0,002303
	160	2421,29	99,5	9899,46	99,260663	0,057282
	220	3415,71	119,9	14375,7	119,198677	0,491853
	280	4322,62	133,77	17893,9	135,105725	1,784162
	360	5556,48	153,75	2364,16	154,413883	0,440740
	400	6232,79	165,19	27289,07	164,143007	1,096195
					SUM	**3,872536**

a = 1,572429
b = 0,531968

	mAs	MPV	SD	SD²	mAs	(mAs-SD)²
Stiglbauer	8	322	39	1492	34,626336	19,128937
	14	735	54	2891	52,315431	2,837772
	25	1169	66	4371	65,977770	0,000494
	40	1910	82	6667	84,335718	5,455579
	71	3680	116	13570	117,064378	1,132901
	110	5149	136	18496	138,473085	6,116148
	160	7720	169	28561	169,557213	0,310487
	200	10366	199	39468	196,478898	6,355954
	250	11784	209	43868	209,487373	0,237532
	320	15400	240	57779	239,482778	0,267518
					SUM	**41,843321**

a = 1,929416
b = 0,500021

	mAs	MPV	SD	SD²	mAs	(mAs-SD)²
Wörther-Madl	160	2624	99,47	9894	98,623277	0,716940
	200	3290	110,55	12221	111,469396	0,845289
	220	3522	115,43	13323	115,657966	0,051968
	320	5191	143	20450	142,682052	0,101091
					SUM	**1,715289**

a = 1,390538
b = 0,541333

VIII. MEASUREMENTS

The measurements were made at Confraternität-Privatklinik (Vienna). These practices consisted in make a series of measurements to ensure the effective use of the machine, the amount of dose and image quality of mammograms obtained. After that, we can evaluate this measurements based on these results.

The measurement site was a prepared room for both, the traditional X-rays and mammography, as shown in the next picture.

More specifically, we use the mammography system 3000NOVA from the brand SIEMENS.

At the time of start with the measurements, the first thing we did was validate the sheets that we will use. For this, the machine had to read the bar code that identified each sheet film. This helps to know what picture corresponds with what sheet.

Next step was to take the mammograms. In this case we used also a dosimeter. The dosimeter can, for instance, measure the entrance dose. To take these measures we changed the thickness for the mammography in every shot. From 20 to 70mm.

The results that we had obtained are shown in the tables below:

AEC-Einstellungen						
PMMA (mm)	**angez. Dicke (mm)**	**Anode/Filter**	**KV**	**mAs**	**CR:Korr.-Schalter**	**CR:Kass.-ID**
20		Mo/Mo	26	18,7	-0,6	923c
30		Mo/Mo	27	34,1	-0,6	916c
40		Mo/Mo	27	71,8	-0,6	923c
45		Mo/Rh	27	76,2	-0,6	770c
50		Mo/Rh	27	109	-0,6	180c
60		W/Rh	26	311	-0,6	916c
70		W/Rh	26	589	-0,6	916c

Standard- Einstellungen							
Anode/Filter	**KV**	**mAs**	**Angez. Eintr.-dosis (mGy)**	**Angez. Dosis-Ind.bzw. AGD (mGy)**	**HVL (Dosim) (ms)**	**Bel.-Zeit (Dosim) (ms)**	**Eintr-dosis (Dosim) (mGy)**
Mo/Mo	26	20		?	0,34	139	1,455
Mo/Mo	27	36		?	0,355	256	3,115
Mo/Mo	27	71		?	0,354	501	6,43
Mo/Rh	27	80		?	0,403	564	6,252
Mo/Rh	27	110		?	0,405	774	8,693
W/Rh	26	320		?	0,513	1721	9,556
W/Rh	26	560		?	0,516	2012	17,37

After obtaining the first results, we put the data on an Excel provided by Mr. Hummel. With that Excel we calculated AGD and we included these results in the table above where we had been collecting all data.

The results are:

Anoden Filter Kombination: MO/MO								
PMMA [mm]	**entspr. Brustdicke [mm]**		**HVL [mmAl]**	**g-factor**	**c-factor**	**s-Wert**	**Gemessene Luftkerma [mGy]**	**AGD [mGy]**
20	20		**0,34**	0,407786	0,894676	1	**1,455**	**0,531**
30	30	1,5	**0,355**	0,294652	0,942778		**3,115**	**0,865**
40	40		**0,354**	0,209451	1,04128		**6,430**	**1,402**

Anoden Filter Kombination MO/RH								
PMMA [mm]	entspr. Brustdicke [mm]		HVL [mmAl]	g-factor	c-factor	s-Wert	Gemessene Luftkerma [mGy]	AGD [mGy]
45	50		0,403	0,201244	1,101872	1,017	6,252	1,410
50	60		0,405	0,176161	1,153284		8,693	1,80

Anoden Filter Kombination W/RH								
PMMA [mm]	entspr. Brustdicke [mm]		HVL [mmAl]	g-factor	c-factor	s-Wert	Gemessene Luftkerma [mGy]	AGD [mGy]
60	75		0,513	0,175745	1,221227	1,042	9,556	2,137
70	90		0,516	0,158464	1,264618		17,37	3,63

Finally the complete table is:

Standard- Einstellungen							
Anode/Filter	KV	mAs	Angez. Eintr.-dosis (mGy)	Angez. Dosis-Ind.bzw. AGD (mGy)	HVL (Dosim) (ms)	Bel.-Zeit (Dosim) (ms)	Eintr-dosis (Dosim) (mGy)
Mo/Mo	26	20		0,531	0,34	139	1,455
Mo/Mo	27	36		0,865	0,355	256	3,5
Mo/Mo	27	71		1,402	0,354	501	6,43
Mo/Rh	27	80		1,410	0,403	564	6,252
Mo/Rh	27	110		1,800	0,405	774	8,693
W/Rh	26	320		2,137	0,513	1721	9,556
W/Rh	26	560		3,630	0,516	2012	17,37

With these results we saw that the image is poor, since these do not look like to limit values. To have a better image we can only increase the dose, however we cannot exced the limit values given by the EU guidelines. So we had to modify the mAs values.

As the machine has a prefixed data, not all of these values are possible. The last ones cannot be measure because they are very high values. That fact implying that the mammography would take a long time and the patient's chest could be moved. In these cases we kept the mAs and we increased the value of KV.

Next, we do the CNR measurements with the dosimeter also. And we get the following results:

	KV	mAs	B-Dose	Time	HVL	AGD
Mo-Mo	26	32	2,326	219,3	0,347	0,85
	27	56	4,834	395,6	0,359	1,34
	27	90	8,177	633,8	0,354	1,28
Mo-Rh	27	125	9,748	878,6	0,405	2,16
	27	160	12,4	1124	0,416	2,52
W-Rh	28	320	11,71	1850	0,542	2,64
	28	560	21,12	3240	0,54	4,4

Below, were performed 16 measurements with CDMAM 50mm. The parameters which we had already obtained were measured again, but this time we measured CNR and we changed the thickness in each mammography.

Finally a comparison is made between the results of the mammographies for 50mm, 60mm and 70mm. For these measurements it used the dosimeter because we wanted to know also the entrance dose.

The results that we obtained are shown in the following table:

		KV	E-Dose	HVL	AgD	mAs
50mm	Mo-Rh	26	7,276	0,387	?	100
		27	8,358	0,4	?	100
		28	9,44	0,412	?	100
		29	10,59	0,423	?	100
	W-Rh	26	2,973	0,525	?	100
		27	3,316	0,538	?	100
		28	3,648	0,55	?	100
		29	3,985	0,56	?	100
		30	4,319	0,569	?	100
60mm	W-Rh	26	3,146	0,513	?	100
		27	3,52	0,524	?	100
		28	3,876	0,535	?	100
		29	4,248	0,544	?	100
		30	4,599	0,553	?	100
70mm	W-Rh	26	3,136	0,509	?	100
		27	3,496	0,523	?	100
		28	3,864	0,532	?	100
		29	4,225	0,541	?	100
		30	4,587	0,549	?	100

We have to re-enter the data obtained on this occasion in the Excel from Mr. Hummel and thereby estimate AgD for this occasion.

The following table shows the results:

Anoden Filter Kombination MO/RH								
PMMA [mm]	entspr. Brustdicke [mm]	KV	HVL [mmAl]	g-factor	c-factor	s-Wert	Gemessene Luftkerma [mGy]	AGD [mGy]
50	60	26	0,387	0,168669	1,155071	1,017	7,276	1,441646
	60	27	0,4	0,174080	1,153780	1,017	8,358	1,707242
	60	28	0,412	0,179074	1,152588	1,017	9,44	1,981530
	60	29	0,423	0,183653	1,151496	1,017	10,59	2,277595

Anoden Filter Kombination W/RH								
PMMA [mm]	entspr. Brustdicke [mm]	KV	HVL [mmAl]	g-factor	c-factor	s-Wert	Gemessene Luftkerma [mGy]	AGD [mGy]
50	60	26	0,525	0,226105	1,141368	1,042	2,973	0,799463
	60	27	0,538	0,231516	1,140077	1,042	3,316	0,912004
	60	28	0,55	0,236510	1,138885	1,042	3,648	1,023887
	60	29	0,56	0,240672	1,137892	1,042	3,985	1,137163
	60	30	0,569	0,244418	1,136998	1,042	4,319	1,250672
60	75	26	0,513	0,175745	1,221227	1,042	3,146	0,703569
	75	27	0,524	0,179464	1,219600	1,042	3,52	0,802798
	75	28	0,535	0,183184	1,217974	1,042	3,876	0,901106
	75	29	0,544	0,186226	1,216642	1,042	4,248	1,002897
	75	30	0,553	0,189269	1,215311	1,042	4,599	1,102298
70	90	26	0,509	0,156489	1,265747	1,042	3,136	0,647253
	90	27	0,523	0,160438	1,263488	1,042	3,496	0,738445
	90	28	0,532	0,162977	1,262035	1,042	3,864	0,828139
	90	29	0,541	0,165516	1,260583	1,042	4,225	0,918557
	90	30	0,549	0,167773	1,259291	1,042	4,587	1,009821

So, we can complete the above table:

			E-Dose	HVL	AgD	mAs
50mm	Mo-Rh	26	7,276	0,387	1,441646	100
		27	8,358	0,4	1,707242	100
		28	9,44	0,412	1,981530	100
		29	10,59	0,423	2,277595	100
	W-Rh	26	2,973	0,525	0,799463	100
		27	3,316	0,538	0,912004	100
		28	3,648	0,55	1,023887	100
		29	3,985	0,56	1,137163	100
		30	4,319	0,569	1,250672	100
60mm	W-Rh	26	3,146	0,513	0,703569	100
		27	3,52	0,524	0,802798	100
		28	3,876	0,535	0,901106	100
		29	4,248	0,544	1,002897	100
		30	4,599	0,553	1,102298	100
70mm	W-Rh	26	3,136	0,509	0,647253	100
		27	3,496	0,523	0,738445	100
		28	3,864	0,532	0,828139	100
		29	4,225	0,541	0,918557	100
		30	4,587	0,549	1,009821	100

So far the measurements were made in manual mode. Now, we will do some measurements automatically. So now, what changes is the "mAs". It was measured with sheets of 18*24cm and sheets of 24*30cm.

Here it is shown the table with the results:

Je 1 AEC-Aufnahmen des WT-Blocks mit jeder weiteren Kassette					
Format (cm*cm)	**Korrektur-schalterstellung**	**Kassetten-ID**	**Anode/Filter**	**KV**	**mAs**
18*24	-0,6	A30271197C	Mo-Rh	27	107
		A30270916C	Mo-Rh	27	11
		A30270923C	Mo-Rh	27	108
		A30270886C	Mo-Rh	27	109
		A30271180C	Mo-Rh	27	109
		A30270770C	Mo-Rh	27	109
		A30270893C	Mo-Rh	27	109
		A30270909C	Mo-Rh	27	108

Je 1 AEC-Aufnahmen des WT-Blocks mit jeder weiteren Kassette					
Format (cm*cm)	**Korrektur-schalterstellung**	**Kassetten-ID**	**Anode/Filter**	**KV**	**mAs**
24*30	-0,6	A30247598C	Mo-Rh	27	112
		A30447604C	Mo-Rh	27	110
		A30247611C	Mo-Rh	27	107
		A30247727C	Mo-Rh	27	109

With these latest measurements is concluded the practical part of the project. From now we have to analyze and use this measurements for others applications.

IX. CNR RESULTS

Before going on to check the images and the values obtained experimentally, we will draw the graphs CNR ² / AGD against KV 50, 60 and 70mm with the database that has the AKH (Allgemeines Krankenhaus der Stadt Wien).

The values of this database are reflected in the following tables, which are separated by location of the experiment.

Diagnosticum						
mm		**KV**	**CNR**	**CNR²**	**AgD**	**CNR²/AgD**
50	W/Al	32	6,03	36,3609	0,82	44,342561
60	W/Al	35	5,7	32,49	1,18	27,533898
70	W/Al	35	5,59	31,2481	1,37	22,808832

Doebling						
mm		**KV**	**CNR**	**CNR²**	**AgD**	**CNR²/AgD**
50	W/Rh	28	11,99	143,7601	1,79	80,312905
60	W/Rh	30	11,24	126,3376	2,35	53,760681
70	W/Rh	30	12,85	165,1225	4,1	40,273780

Doringer						
mm		**KV**	**CNR**	**CNR²**	**AgD**	**CNR²/AgD**
50	W/Rh	28	7,96	63,3616	1,06	59,775094
60	W/Rh	32	6,96	48,4416	1,3	37,262769
70	W/Rh	32	5,44	29,5936	1,74	17,007816

DZ_Brigittenau						
mm		**KV**	**CNR**	**CNR²**	**AgD**	**CNR²/AgD**
50	W/Al	32	4,95	24,5025	0,57	42,986842
60	W/Al	32	4,76	22,6576	0,83	27,298313
70	W/Al	32	4,88	23,8144	1,1	21,649455

DZ_Margareten						
mm		**KV**	**CNR**	**CNR²**	**AgD**	**CNR²/AgD**
50	W/Rh	29	7,96	63,3616	8,45	7,498414
60	W/Rh	31	6,96	48,4416	8,02	6,040100
70	W/Rh	30	5,44	29,5936	8,46	3,498061

DZ_Meidling						
mm		**KV**	**CNR**	**CNR²**	**AgD**	**CNR²/AgD**
50	Rh/Rh	29	14,68	215,5024	1,4	153,930286
60	Rh/Rh	30	10,79	116,4241	1,42	81,988803
70	Rh/Rh	30	9,17	84,0889	1,89	44,491481

DZ_Hernals						
mm		**KV**	**CNR**	**CNR²**	**AgD**	**CNR²/AgD**
50	W/Rh	30	7,04	49,5616	1,51	32,8222517
60	W/Rh	31	6,18	38,1924	1,64	23,2880488
70	W/Rh	32	5,38	28,9444	2,46	11,7660163

Frühwald_mammo1						
mm		**KV**	**CNR**	**CNR²**	**AgD**	**CNR²/AgD**
50	Rh/Rh	29	15,43	238,0849	1,5	158,723267
60	Rh/Rh	29	14,44	208,5136	2,23	93,5038565
70	Rh/Rh	31	13,05	170,3025	3,25	52,4007692

Frühwald_mammo2						
mm		**KV**	**CNR**	**CNR²**	**AgD**	**CNR²/AgD**
50	Rh/Rh	29	17,12	293,0944	1,46	200,749589
60	Rh/Rh	29	14,62	213,7444	1,74	122,841609
70	Rh/Rh	30	10,99	120,7801	1,77	68,2373446

Hanusch						
mm		**KV**	**NR**	**CNR²**	**AgD**	**CNR²/AgD**
50	Mo/Mo	31	4,75	22,5625	1,43	15,777972
60	Mo/Rh	32	3,9	15,21	1,58	9,62658228
70	Mo/Rh	33	3,08	9,4864	2,26	4,19752212

Hietzing						
mm		**KV**	**CNR**	**CNR²**	**AgD**	**CNR²/AgD**
50	W/Al	32	6,18	38,1924	0,84	45,4671429
60	W/Al	35	5,95	35,4025	1,33	26,6184211
70	W/Al	35	5,5	30,25	1,44	21,0069444

Hollenstein						
mm		**KV**	**CNR**	**CNR²**	**AgD**	**CNR²/AgD**
50	Rh/Rh	28	9,41	88,5481	1,16	76,334569
60	Rh/Rh	32	7,64	58,3696	1,47	39,7072109
70	Rh/Rh	32	7,42	55,0564	2,41	22,8449793

KH_Hietzing						
mm		**KV**	**CNR**	**CNR²**	**AgD**	**CNR²/AgD**
50	W/Rh	30	7,44	55,3536	1,06	52,2203774
60	W/Rh	31	6,64	44,0896	1,47	29,9929252
70	W/Rh	32	5,95	35,4025	2,09	16,9389952

Kubin						
mm		**KV**	**CNR**	**CNR²**	**AgD**	**CNR²/AgD**
50	Mo/Rh	28	7,61	57,9121	2,54	22,8000394
60	Mo/Rh	30	7,44	55,3536	3,65	15,1653699
70	Mo/Rh	30	7,29	53,1441	7,16	7,42236034

Liesing						
mm		**KV**	**CNR**	**CNR²**	**AgD**	**CNR²/AgD**
50	W/Al	35	6,08	36,9664	0,97	38,109691
60	W/Al	38	5,75	33,0625	1,56	21,19391
70	W/Al	38	5,46	29,8116	1,72	17,332326

Linhart						
mm		**KV**	**CNR**	**CNR²**	**AgD**	**CNR²/AgD**
50	W/Rh	30	6,45	41,6025	1,17	35,5576923
60	W/Rh	31	6,08	36,9664	1,68	22,0038095
70	W/Rh	32	5,28	27,8784	2,16	12,9066667

Nics						
mm		KV	CNR	CNR²	AgD	CNR²/AgD
50	W/Rh	31	10,07	101,4049	1,87	54,227219
60	W/Ag	31	9,47	89,6809	2,6	34,492654
70	W/Ag	34	7,21	51,9841	2,7	19,25337

Roentgen_Mistelbach						
mm		KV	CNR	CNR²	AgD	CNR²/AgD
50	Mo/Rh	28	12,59	158,5081	4,95	32,0218384
60	Mo/Rh	28	12,26	150,3076	7,9	19,0262785
70	W/Rh	30	7,11	50,5521	3,95	12,798

Salk						
mm		KV	CNR	CNR²	AgD	CNR²/AgD
50	Rh/Rh	29	7,4	54,76	1,1	49,781818
60	Rh/Rh	29	6,51	42,3801	1,37	30,93438
70	Rh/Rh	30	5,35	28,6225	1,55	18,466129

Schahbasi						
mm		KV	CNR	CNR²	AgD	CNR²/AgD
50	Rh/Rh	29	9,22	85,0084	1,37	62,049927
60	Rh/Rh	30	8,53	72,7609	1,6	45,4755625
70	Rh/Rh	30	6,2	38,44	1,75	21,9657143

Schillerpark						
mm		KV	CNR	CNR²	AgD	CNR²/AgD
50	Rh/Rh	29	18,18	330,5124	1,78	185,68112
60	Rh/Rh	29	14,45	208,8025	1,84	113,47962
70	Rh/Rh	31	10,76	115,7776	1,96	59,070204

Urfahr						
mm		KV	CNR	CNR²	AgD	CNR²/AgD
50	W/Rh	30	6,79	46,1041	1,08	42,6889815
60	W/Rh	31	5,7	32,49	1,84	17,6576087
70	W/Rh	32	5,02	25,2004	1,82	13,8463736

Wagner						
mm		KV	CNR	CNR²	AgD	CNR²/AgD
50	W/Rh	30	6,67	44,4889	1,34	33,200672
60	W/Rh	31	5,83	33,9889	1,73	19,646763
70	W/Rh	32	4,9	24,01	2,18	11,013761

Walter						
mm		KV	CNR	CNR²	AgD	CNR²/AgD
50	W/Ag	30	7,47	55,8009	1,59	35,0949057
60	W/Ag	29	6,7	44,89	1,72	26,0988372
70	W/Ag	30	5,75	33,0625	2,11	15,6694313

Wiesmayr						
mm		KV	CNR	CNR²	AgD	CNR²/AgD
50	Rh/Rh	29	9,03	81,5409	1,24	65,75879
60	Rh/Rh	29	7,05	49,7025	1,27	39,135827
70	Rh/Rh	30	6,04	36,4816	1,55	23,536516

Wolfsberg						
mm		KV	CNR	CNR²	AgD	CNR²/AgD
50	W/Rh	30	10,72	114,9184	1,4	82,0845714
60	W/Rh	31	9,14	83,5396	1,78	46,9323596
70	W/Rh	32	7,41	54,9081	2,24	24,5125446

With these data we obtain the graphs according to the thickness of the chest and the type of anode used.

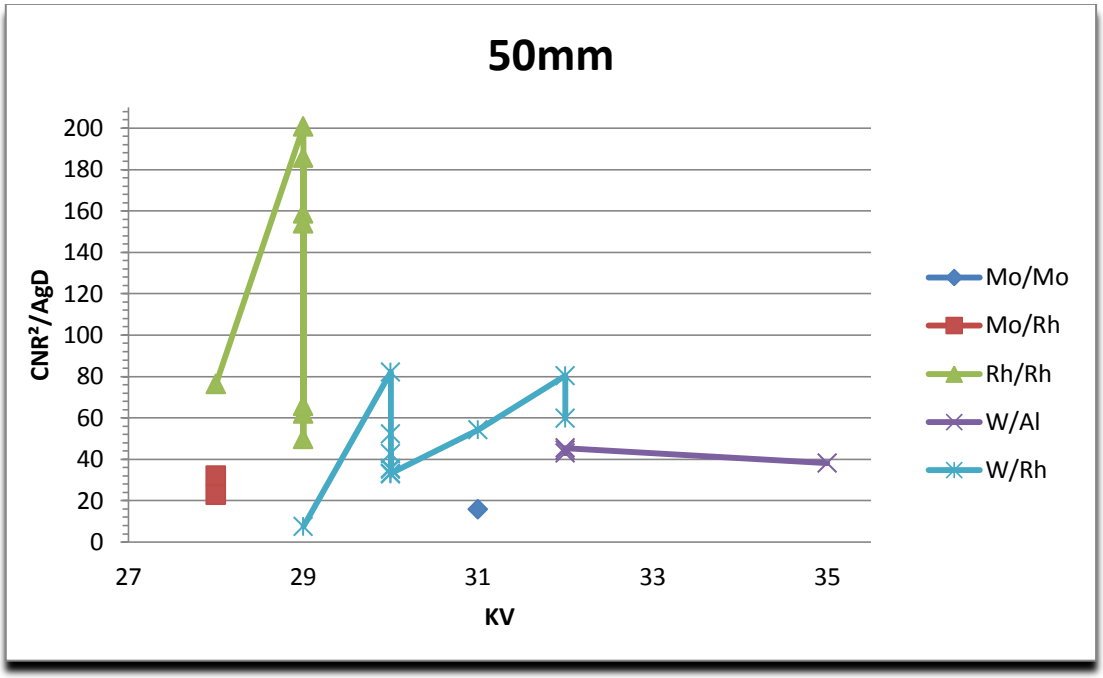

In this first graph corresponding to 50mm we can observe that when the anode used is Rh/Rh the range of CNR^2/AgD is much larger than the range in other anodes when we use a same KV, which it means that the quality of the image could be better.

The anodes of Mo/Rh and W/Al kept less difference of $CNR2^2/AgD$ even when KV values are different, so the probability of having a good image remains.

In the case of Mo/Mo although the value of CNR^2/AGD is not high (not good quality image), we cannot say anything concrete because we only have a data.

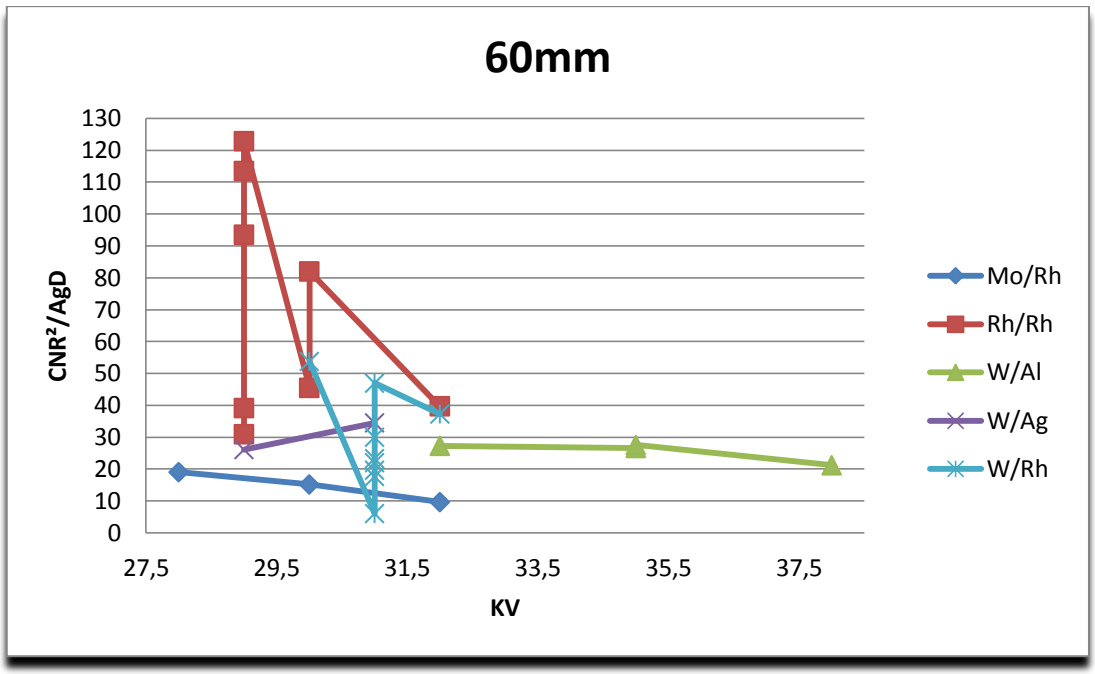

In this graph, corresponding to 60mm, we can see that the anode of Rh/Rh has the highest range of values for the same KV. This means that the probability of having a good image is increased.

The anode of W/Rh, however has a narrower range for the same value of KV, coinciding many of its points around the 20 CNR²/AGD. Besides these values are lower, so we don't have a really good quality image.

Moreover, the anodes of W/W, Mo/Rh and W/Al have values of CNR²/AGD similar along different KV values. The value of CNR²/AGD tends to descend as increases the KV in the cases of W/Al and Mo/Rh and increase in the case of W/Ag.

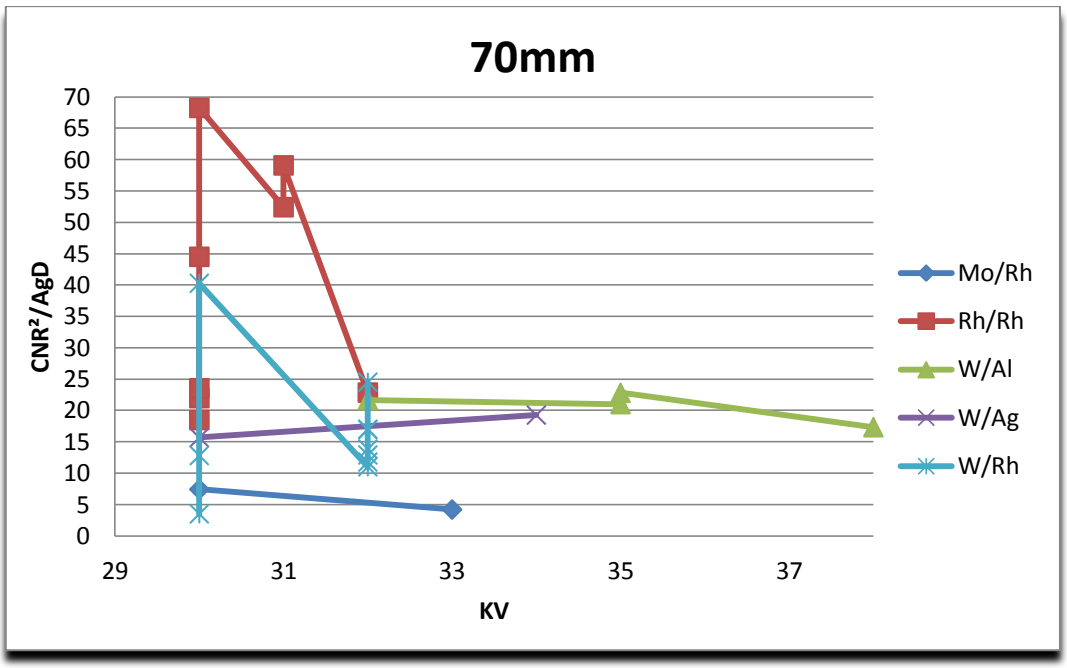

Finally, in the graphic corresponding to 70mm it is observed that the general trend is very similar to the results obtained with the graphic of 60mm. The anode of Rh/Rh presents the more dispersion data and the highest values for CNR^2/AGD regarding the same KV. That means, we can achieve the best quality image.

The next anode is the anode of W/Rh which has lower dispersion than the anode of Rh/Rh for the same value of KV, but still one of the higher values.

Therefore we can also say that the anodes of W/Al and Mo/Rh present a small downward in front of a higher value of KV, as happened with the 60mm's graph.

Finally, we notice that the anode of W/Ag continues an upward trend for higher KV values, although the difference is less than for other anodes.

In the experiments we obtained some pictures. An example of theme is shown below.

50mm:

60mm:

70mm:

As we are interested in the graphics of CNR ² / AGD against KV for 50mm, 60 and 70mm, we get these data and we draw their graphs.

To find the data we have taken measures of the MPV and SD in the background and the object (small square seen in the images) using the “ImageJ” program for each of the images. We have nine samples for the case of 50mm and five samples for the thicknesses of 60mm and 70mm.

The data are compiled in the following tables:

	50mm			
	MPV (Backgrd)	**SD** (Backgrd)	**MPV** (Object)	**SD** (Object)
Mo-Rh	509,919238	6,6833465	469,597222	7,231312
	538,645817	6,8771861	506,003902	6,917681
	540,697739	5,9997944	506,518189	6,396514
	526,951987	5,0639464	494,064306	5,323411
W-Rh	500,734551	7,4667395	469,370606	7,993560
	514,001936	6,8215789	483,569665	7,264591
	522,290205	6,9600918	493,985296	7,247594
	530,554085	6,5176467	500,457042	6,716519
	525,911524	5,5150101	497,288652	5,826509

	60mm			
	MPV (Backgrd)	**SD** (Backgrd)	**MPV** (Object)	**SD** (Object)
W-Rh	415,022591	9,909837	385,212772	10,43835
	409,188675	9,171612	380,789776	9,778358
	433,33346	9,163876	406,112268	9,398121
	408,115375	7,807578	379,974358	8,150297
	421,09847	8,05619	395,261659	8,372774

	70mm			
	MPV (Backgrd)	**SD** (Backgrd)	**MPV** (Object)	**SD** (Object)
W-Rh	408,570692	12,387294	380,551706	12,638801
	387,17919	11,347783	361,099605	11,729094
	394,975869	10,736315	368,105586	11,162601
	411,91021	10,764251	386,961168	11,146797
	407,67092	10,327374	383,577517	10,530819

With this information and with the help of the formulas and the experimental data obtained by making measurements, we draw the table below:

$$CNR = \frac{\text{mean pixel value (signal)} - \text{mean pixel value (background)}}{\sqrt{\frac{\text{Standar deviation (signal)}^2 + \text{Standard deviation (background)}^2}{2}}}$$

	50mm								
	KV	AgD	MPV (Backgrd)	SD (Backgrd)	MPV (Object)	SD (Object)	CNR	CNR²	CNR²/AgD
Mo-Rh	26	1,44	509,91924	6,6833465	469,59722	7,231312	5,791128	33,537167	23,289699
	27	1,71	538,64582	6,8771861	506,00390	6,917681	4,732452	22,396105	13,097137
	28	1,98	540,69774	5,9997944	506,51819	6,396514	5,511651	30,378294	15,342573
	29	2,28	526,95199	5,0639464	494,06431	5,323411	6,330277	40,072410	17,575618
W-Rh	26	0,8	500,73455	7,4667395	469,37061	7,993560	4,054999	16,443018	20,553773
	27	0,91	514,00194	6,8215789	483,56967	7,264591	4,318737	18,651489	20,496142
	28	1,02	522,29021	6,9600918	493,98530	7,247594	3,983635	15,869345	15,558182
	29	1,14	530,55409	6,5176467	500,45704	6,716519	4,547872	20,683138	18,143103
	30	1,25	525,91152	5,5150101	497,28865	5,826509	5,045547	25,457543	20,366034

	60mm								
	KV	AgD	MPV (Backgrd)	SD (Backgrd)	MPV (Object)	SD (Object)	CNR	CNR²	CNR²/AgD
W-Rh	26	0,7	415,02259	9,909837	385,21277	10,43835	2,928985	8,578954	12,255649
	27	0,8	409,18868	9,171612	380,78978	9,778358	2,995715	8,974307	11,217884
	28	0,9	433,33346	9,163876	406,11227	9,398121	2,932769	8,601134	9,556816
	29	1	408,11538	7,807578	379,97436	8,150297	3,526100	12,433379	12,433379
	30	1,1	421,09847	8,05619	395,26166	8,372774	3,144692	9,889087	8,990079

	70mm								
	KV	AgD	MPV (Backgrd)	SD (Backgrd)	MPV (Object)	SD (Object)	CNR	CNR²	CNR²/AgD
W-Rh	26	0,65	408,57069	12,387294	380,55171	12,638801	2,239069	5,013428	7,712966
	27	0,74	387,17919	11,347783	361,09961	11,729094	2,259927	5,107269	6,901715
	28	0,83	394,97587	10,736315	368,10559	11,162601	2,453564	6,019975	7,252982
	29	0,92	411,91021	10,764251	386,96117	11,146797	2,276955	5,184526	5,635355
	30	1,01	407,67092	10,327374	383,57752	10,530819	2,310100	5,336563	5,283725

Consequently the graphs obtained are:

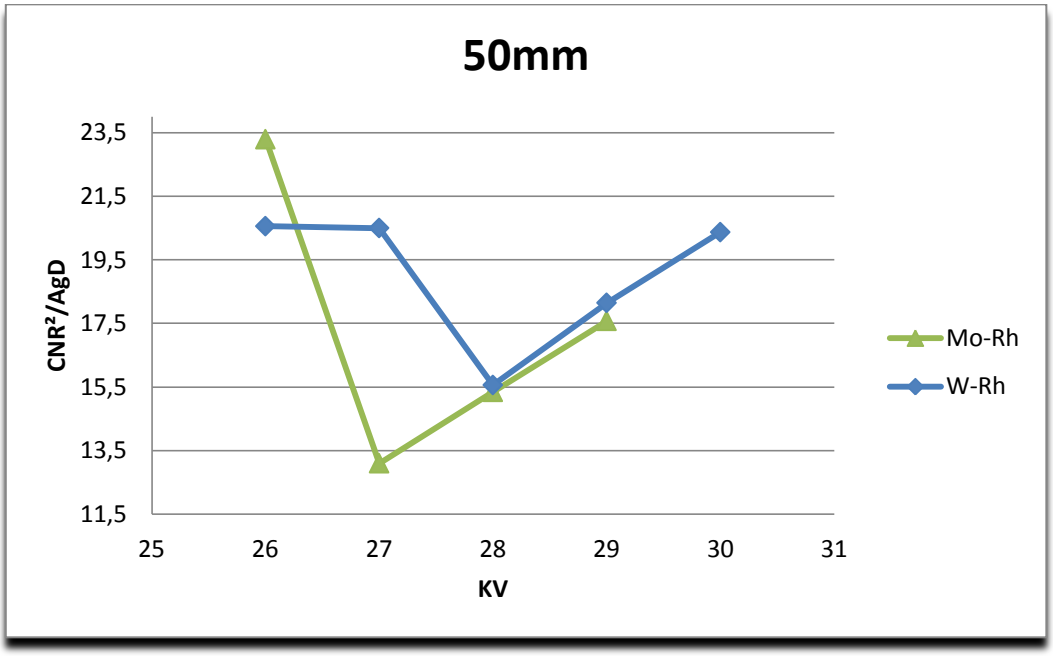

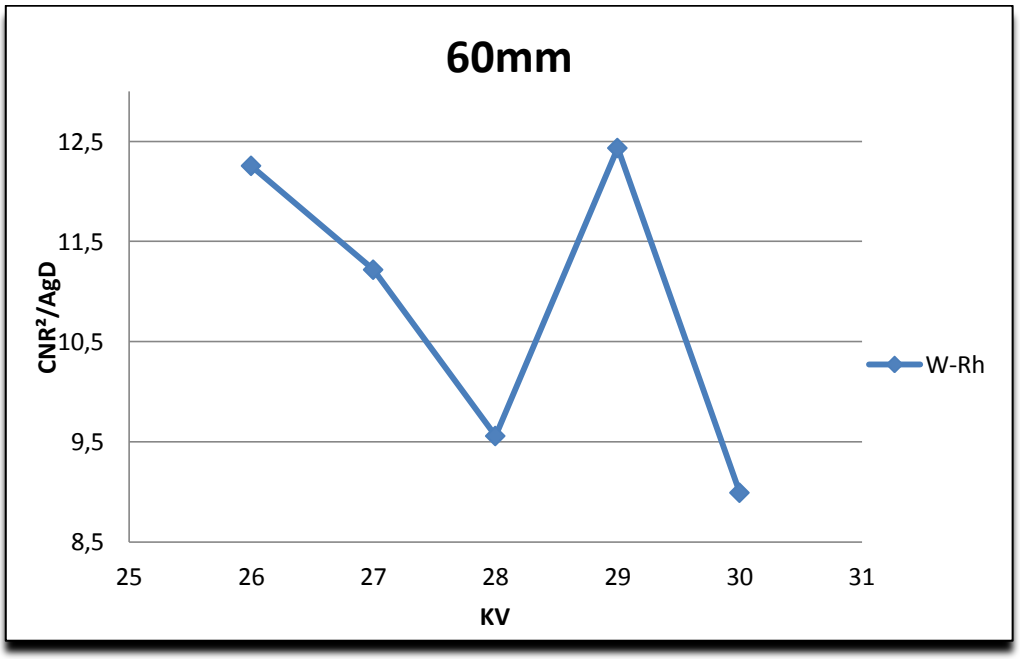

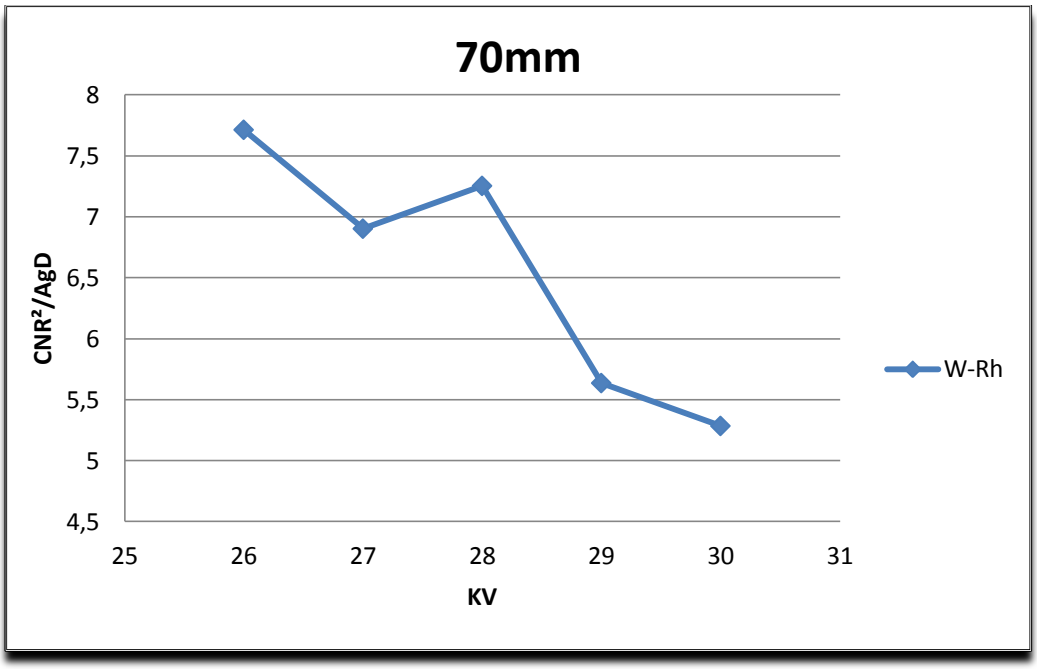

In these plots we can observe the behavior of the noise for the anodes of Mo/Rh and W/Rh in the case of 50mm and W/Rh in the case of 60mm and 70mm.

In the 50mm's plot, the chart shows that the anode of Mo/Rh has a larger dispersion of values on the y axis (CNR^2/AGD), so the image quality variation is greater than for the anode of W/Rh.

The CNR^2/AGD values suffer a decrease for a particular kV value, and then returns to increase as the value of KV is increasing.

We see that for the case of 60mm the graph follows the same form that for the graphic of 50mm. Although in this case, it is shown another decline in the value of CNR^2/AGD for the highest value of KV. The image quality in those cases is difficult to obtend and is very relationated with the KV.

We note that as the thickness increase the difference between the values of CNR^2/AGD becomes smaller. For this reason the graph of 70mm is which present the lower amplitude of CNR^2/AGD, the worst image quality.

Moreover, except in one point of the graph, the trend is downward all the time. That is, for higher values of KV the CNR^2/AGD, image quality, values decrease.

X. SNR RESULTS

Finally we obtained the plots of SNR with the images that we take in the experiment and we checked and analyzed if they are a good and beneficial results.

The SNR values are:

$$SNR = \frac{Mean\ Pixel\ Value(signal)}{Standard\ Deviation\ (signal)}$$

	50mm								
	KV	**AgD**	**MPV** (Backgrd)	**SD** (Backgrd)	**MPV** (Object)	**SD** (Object)	**MPVo/SDo** SNR	**SNR²**	SNR²/AgD
Mo-Rh	26	1,44	509,91924	6,683347	469,59722	7,231312	64,939422	4217,12851	2928,561464
	27	1,71	538,64582	6,877186	506,00390	6,917681	73,146466	5350,4055	3128,892105
	28	1,98	540,69774	5,999794	506,51819	6,396514	79,186604	6270,51831	3166,92844
	29	2,28	526,95199	5,063946	494,06431	5,323411	92,809724	8613,64490	3777,914431
W-Rh	26	0,8	500,73455	7,466740	469,37061	7,993560	58,718593	3447,87315	4309,841439
	27	0,91	514,00194	6,821579	483,56967	7,264591	66,565300	4430,93917	4869,163926
	28	1,02	522,29020	6,960092	493,98530	7,247594	68,158523	4645,5842	4554,494313
	29	1,14	530,55408	6,517647	500,45704	6,716519	74,511369	5551,94417	4870,126461
	30	1,25	525,91152	5,515010	497,28865	5,826509	85,349336	7284,50909	5827,60727

	60mm								
	KV	**AgD**	**MPV** (Backgrd)	**SD** (Backgrd)	**MPV** (Object)	**SD** (Object)	**MPVo/SDo** SNR	**SNR²**	SNR²/AgD
W-Rh	26	0,7	415,02259	9,909837	385,21277	10,43835	36,903608	1361,87625	1945,537502
	27	0,8	409,18868	9,171612	380,78978	9,778358	38,942098	1516,48700	1895,608751
	28	0,9	433,33346	9,163876	406,11227	9,398121	43,212071	1867,28304	2074,758938
	29	1	408,11538	7,807578	379,97436	8,150297	46,620922	2173,51034	2173,510337
	30	1,1	421,09847	8,05619	395,26166	8,372774	47,207969	2228,59238	2025,99307

	70mm								
	KV	AgD	MPV (Backgrd)	SD (Backgrd)	MPV (Object)	SD (Object)	MPVo/SDo SNR	SNR²	SNR²/AgD
W-Rh	26	0,65	408,57069	12,387294	380,55171	12,638801	30,109795	906,59975	1394,768845
	27	0,74	387,17919	11,347783	361,09961	11,729094	30,786658	947,81831	1280,835551
	28	0,83	394,97587	10,736315	368,10559	11,162601	32,976686	1087,46181	1310,194948
	29	0,92	411,91021	10,764251	386,96117	11,146797	34,715010	1205,13191	1309,92599
	30	1,01	407,67092	10,327374	383,57752	10,530819	36,424282	1326,72829	1313,592368

The respective graphics are:

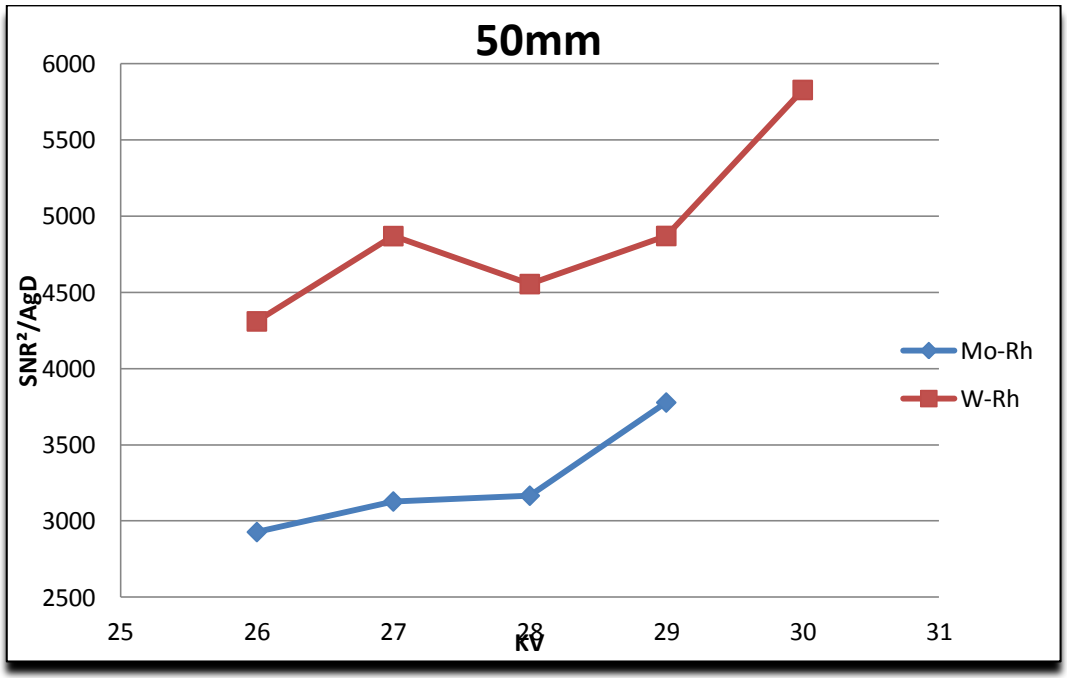

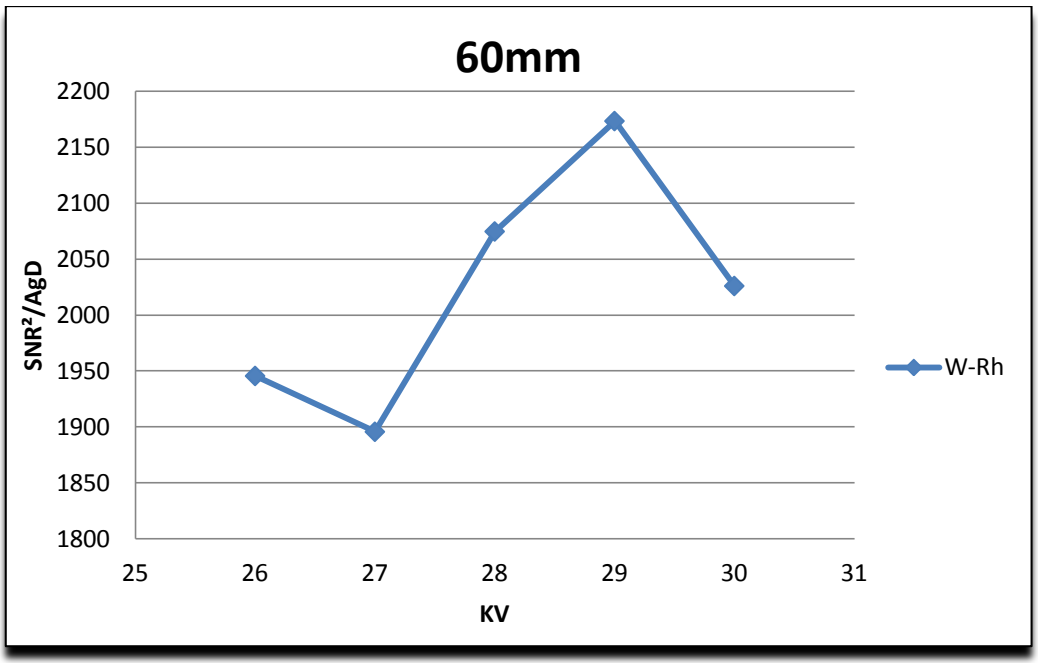
60mm
2200
2150
2100
2050
2000
1950
1900
1850
1800
SNR²/AgD
25
26
27
28
29
30
31
KV
W-Rh

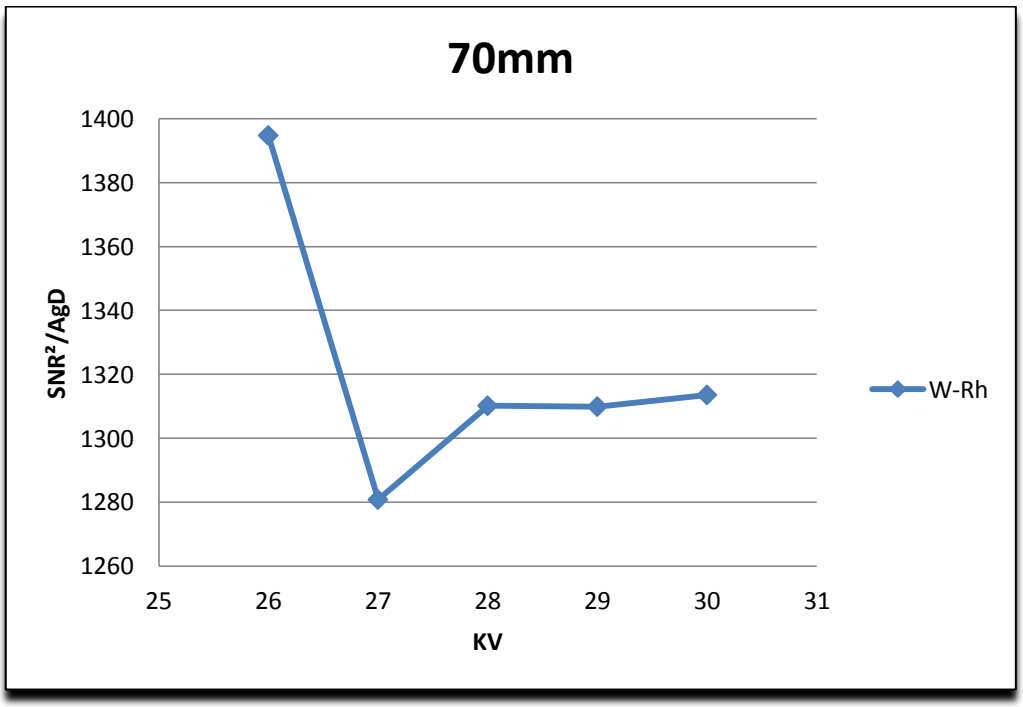
70mm
1400
1380
1360
1340
1320
1300
1280
1260
SNR²/AgD
25
26
27
28
29
30
31
KV
W-Rh

In these graphs you can see SNR^2/AGD against KV for a 50mm, 60mm and 70mm thicknesses.

The graph of 50mm, the SNR^2/AGD value tends to increase with the KV increasing, which means that the image quality will be better for a higher KV.

We can also observe that in the 50mm plot the W/Rh anode has higher image quality than the Mo/Rh anode, since for the same values of KV the W/Rh anode curve is always above.

In the graph of 60mm, however, for very high values of KV the curve undergoes a decline, so we get the best pictures in the intermediate values of KV.

Finally, in the graph of 70mm, we noted that we obtain the best image quality for the lowest value of KV. Higher values of KV get lost image quality.

XI. FINAL CONCLUSIONS

In this project we can see all the process that we have followed to get the CNR and the SNR plots. Besides we can read wich was the method that we used and all the operations that we have to do. As a result we get both graphics for three different thicknesses and we can compare them.

We have observed in the different graphs, that the maximum values for CNR^2/AGD and SNR^2/AGD decreased while the breast thickness increased. This makes sense because the dose remains is the same, but the breast size is bigger, so the image quality may not be as good. However, it has been get quite acceptable values for 60mm to 70mm, which means that the method used is quite reliable for a bigger breast.

It has also been found that these graphs follow a trend. That is, the KV value, that we take, influences them.

With the accomplishment of these graphs we can help future researches to get a better image. For that, it should be taken those values that we obtained in our operations, where image quality is acceptable and apply these values in the new measure.

Therefore we can say that the purpose of the experiment was achieved.

XII. REFERENCES

- Data base for the hospital (AKH, Allgemeines Krankenhaus der Stadt Wien).
- Mr. Hummel documents.
- European protocol for the quality control of the physical and technical aspects of mammography screening.
- European guidelines for quality assurance in breast cancer screening and diagnosis.
- www.cancer.org
- Wikipedia (mammogram, cancer…)
- www.fda.gov
- www.krebshilfe.net
- ***Evaluations of software for reading images of the CDMAM test object to assess digital mammography systems***. (Kenneth C. Young, Abdulaziz Alsager, Jennifer M. Oduko, Hilde Bosmans, Beatrijs Verbrugge, Tanya Geertse, Ruben van Engen).
- ***Evaluations of software for reading images of the CDMAM test object to assess digital mammography systems***. (Kenneth C. Young, Abdulaziz Alsager, Jennifer M. Oduko, Hilde Bosmans, Beatrijs Verbrugge, Tanya Geertse, Ruben van Engen)
- ***Comparison of software and human observers in reading images of the CDMAM test object to assess digital mammography systems.*** (Kenneth C. Young, James J.H. Cooka, Jennifer M. Odukoa, Hilde Bosmans).
- ***Image quality assessment in digital mammography: part I. Technical characterization of the systems.*** (N.W.Marshall, P.Monnin, H.Bosmans, F.O.Bochud and F.R.Verdun).

- ***Signal-to-noise ratio, contrast-to-noise ratio and pharmacokinetic modeling considerations in dynamic contrast-enhanced magnetic resonance imaging***. (Xin Li, Wei Huang, William D. Rooney).
- ***Signal-to-noise optimization of medical imaging systems.*** (I.A.Cunningham, Rodney Shaw).
- ***MANUAL Contrast-detail Phantom Artinis CDMAM type 3.4.*** (M.A.O.Thijssen, K.R.Bijkerk, R.J.M van der Burght).
- ***Determination of contrast-detail curves of mammography systems by automated image analysis.*** (N.Karssemeijer, M.A.O.Thijssen)
- ***The Rose model, revisited***. (Arthur E.Burgess).
- ***Quantifying the performance of human and software CDMAM phantom image observes for the qualification of digital mammography systems***. (Lynn Fletcher-Heath, Richard Van Metter).